

Accurate estimation of Li/Ni mixing degree of lithium nickel oxidecathode materials

Penghao Chen(陈鹏浩), Lei Xu(徐磊), Xiqian Yu(禹习谦), and Hong Li(李泓)

Citation: Chin. Phys. B, 2024, 33 (**5**): 058202. DOI: 10.1088/1674-1056/ad3036
Journal homepage: http://cpb.iphy.ac.cn; http://iopscience.iop.org/cpb

What follows is a list of articles you may be interested in

Synthesis and electrochemical performance of La_2CuO_4 as a promising coating material for high voltage Li-rich layered oxide cathodes

Fuliang Guo(郭福亮), Jiaze Lu(卢嘉泽), Meihua Su(苏美华), Yue Chen(陈约), Jieyun Zheng(郑杰允), Liang Yin(尹良), and Hong Li(李泓)

Chin. Phys. B, 2023, 32 (**8**): 088201. DOI: 10.1088/1674-1056/acd2bc

A novel calculation strategy for optimized prediction of the reduction of electrochemical window at anode

Guochen Sun(孙国宸), Jian Gao(高健), and Hong Li(李泓)

Chin. Phys. B, 2023, 32 (**7**): 078201. DOI: 10.1088/1674-1056/accd51

Structural, electronic, and Li-ion mobility properties of garnet-type $Li_7La_3Zr_2O_{12}$ surface: An insight from first-principles calculations

Jing-Xuan Wang(王靖轩), Bao-Zhen Sun(孙宝珍), Mei Li(李梅), Mu-Sheng Wu(吴木生), and Bo Xu(徐波)

Chin. Phys. B, 2023, 32 (**6**): 068201. DOI: 10.1088/1674-1056/acc05d

Stress effect on lattice thermal conductivity of anode material $NiNb_2O_6$ for lithium-ion batteries

Ao Chen(陈奥), Hua Tong(童话), Cheng-Wei Wu(吴成伟), Guofeng Xie(谢国锋), Zhong-Xiang Xie(谢忠祥), Chang-Qing Xiang(向长青), and Wu-Xing Zhou(周五星)

Chin. Phys. B, 2023, 32 (**5**): 058201. DOI: 10.1088/1674-1056/acaa2d

In situ formed FeS_2@CoS cathode for long cycling life lithium-ion battery

Xin Wang(王鑫), Bojun Wang(汪博筠), Jiachao Yang(杨家超), Qiwen Ran(冉淇文), Jian Zou(邹剑), Pengyu Chen(陈鹏宇), Li Li(李莉), Liping Wang(王丽平), and Xiaobin Niu(牛晓滨)

Chin. Phys. B, 2021, 30 (**8**): 088201. DOI: 10.1088/1674-1056/abe9ab

---

Accurate estimation of Li/Ni mixing degree of lithium nickel oxide cathode materials

Penghao Chen(陈鹏浩)[1,2,3], Lei Xu(徐磊)[1,3,†], Xiqian Yu(禹习谦)[1,2,3,‡], and Hong Li(李泓)[1,2,3]

[1] *Institute of Physics, Chinese Academy of Sciences, Beijing* 100190, *China*

[2] *Center of Materials Science and Optoelectronics Engineering, University of Chinese Academy of Sciences, Beijing* 100049, *China*

[3] *Beijing Frontier Research Center on Clean Energy, Huairou Division, Institute of Physics, Chinese Academy of Sciences, Beijing* 101400, *China*

(Received 31 December 2023; revised manuscript received 15 February 2024; accepted manuscript online 5 March 2024)

Li/Ni mixing negatively influences the discharge capacity of lithium nickel oxide and high-nickel ternary cathode materials. However, accurately measuring the Li/Ni mixing degree is difficult due to the preferred orientation of lab-based XRD measurements using Bragg–Brentano geometry. Here, we find that employing spherical harmonics in Rietveld refinement to eliminate the preferred orientation can significantly decrease the measurement error of the Li/Ni mixing ratio. The Li/Ni mixing ratio obtained from Rietveld refinement with spherical harmonics shows a strong correlation with discharge capacity, which means the electrochemical capacity of lithium nickel oxide and high-nickel ternary cathode can be estimated by the Li/Ni mixing degree. Our findings provide a simple and accurate method to estimate the Li/Ni mixing degree, which is valuable to the structural analysis and screening of the synthesis conditions of lithium nickel oxide and high-nickel ternary cathode materials.

Keywords: lithium nickel oxide, high-nickel ternary cathode, Li/Ni mixing, spherical harmonics function, discharge capacity

PACS: 82.47.Aa, 82.45.Fk **DOI:** 10.1088/1674-1056/ad3036

1. Introduction

Lithium ion batteries (LIBs) with high energy density are indispensable for the development of consumer electronics, electric vehicles and electric aircrafts.[1,2] At present, the energy density of LIBs is mainly limited by the cathode materials, of which the ternary cathode is one of the main research objects.[3–5] To pursue higher energy density, ternary cathode materials are developing towards high nickel contents (Ni content $>$ 80%) and ultra-high nickel contents (Ni content $>$ 90%), which present discharge capacities over 200 mAh/g and 220 mAh/g, respectively.[6,7] Nowadays, single-crystallization is an important developing direction of the high-nickel ternary cathode, which has fewer side reactions and better cycle performance.[8–13] However, the preparation of a single crystal high nickel cathode needs sintering at a higher temperature, which easily causes the transformation of the layered structure to a partial rock-salt phase.

It is acknowledged that the degree of completeness of the layered structure is a key factor which limits the electrochemical performance and causes the irreversible capacity loss.[14] Generally, the Li/Ni mixing ratio is the index of the degree of preservation of the layered structure and can be evaluated by the ordinary x-ray diffraction (XRD) experiment. It is reported the intensity ratio of peak_{003} to peak_{104} can reflect the Li/Ni mixing degree.[15] However, the ratio is greatly fluctuant due to the large error values of intensity of peak_{003} and peak_{104} between each lab-based XRD experiment due to the preferred orientation of the samples.[15–18] The split of peak_{006} and peak_{102} also reflects the completeness of the layered structure and Li/Ni mixing, which is only a qualitative approach, not a quantitative one.[19]

The value of Li/Ni mixing degree can be obtained from Rietveld refinement. Nevertheless, the accuracy of Li/Ni mixing degree is influenced by many factors such as the accuracy of peak intensities. The observed peak intensity ratios, which are influenced by both the Li/Ni mixing and the preferred orientation (texture) stemmed from not randomly oriented crystallites, play an important role in the refinement. The preferred orientation is serious for ordinary XRD measurements using Bragg–Brentano geometry and lack of consideration of it will cause great measurement error to the calculated Li/Ni mixing.

In this work, we demonstrate that sample testing inconsistencies cause serious preferred orientation and the inaccurately determination of the Li/Ni mixing ratio. Spherical harmonics functions are used to eliminate the preferred orientation which is favorable to obtain a more accurate Li/Ni mixing degree by Rietveld refinement on ordinary XRD results. The linear correlation between Li/Ni mixing ratio and discharge capacity is applicable for both $LiNiO_2$ (LNO) and $LiNi_{0.92}Co_{0.03}Mn_{0.05}O_2$ (Ni92) cathode, which means the Li/Ni mixing is detrimental to the electrochemistry capacity. These findings provide a method which can accurately determine Li/Ni mixing degree and a simple index — Li/Ni mixing

†Corresponding author. E-mail: leixu@iphy.ac.cn

‡Corresponding author. E-mail: xyu@iphy.ac.cn

© 2024 Chinese Physical Society and IOP Publishing Ltd

ratio to estimate the discharge capacity of lithium nickel oxide and high-nickel ternary cathode materials before electrochemical experiments, which is beneficial for the screening of lithium nickel oxide and high-nickel ternary cathode materials.

2. Experimental details

Materials synthesis LNO and Ni92 cathode materials were prepared by solid-state sintering process. The $Ni(OH)_2$ precursor was provided by Lawa Lithium Energy and Technology Co., LTD. $Ni_{0.92}Co_{0.02}Mn_{0.06}(OH)_2$ precursor was supplied from CNGR Advanced Material Co., Ltd. The precursors were mixed with 4%–6% excess $LiOH{\cdot}H_2O$ by grinding and then sintered at 650 °C–1000 °C for 10 h–70 h by using different sintering procedures. The flow rate of oxygen gas was about 40 sccm–60 sccm. The obtained powder was grinded by mortar & pestle and then stored in a seal.

Materials characterization XRD experiments were conducted by using a flat sample stage on Bruker D8 Advance which uses Cu-$K\alpha$ radiation in Bragg–Brentano geometry. Rietveld refinement of the LNO and Ni92 cathode materials was conducted in TOPAS (v.6) software and based on the R-3m space group with the transition metals atoms on the 3a sites, Li atoms on the 3b sites and O atoms on the 6c sites. The $B_{\rm iso}$ of transition metals, lithium and oxygen atoms were fixed at 0.15, 0.50 and 0.42, respectively. The z coordination of O was refined and the x and y coordinations of O were fixed. The content of Ni^{2+} in LiO_6 layer (Ni_{Li}) was refined and was referred to as Li/Ni mixing. The content of Ni_{Li}, crystallite size and strain were also included in the refinement. The 6th order spherical harmonic function was checked to decrease the error from preferred orientation. All samples were refined with the same procedure and parameter setting. The morphology of samples was characterized by a field emission scanning electron microscope (FE-SEM, S4800, Hitachi) under the accelerating voltage of 10 kV. The Raman spectra were recorded from 300 cm^{-1} to 800 cm^{-1} using a HORIBA LabRAM HR Evolution system which has a deep-depleted thermoelectrically cooled CCD array detector. Excitation of all samples was conducted by a frequency-doubled Nd-YAG laser (at the wavelength of 523 nm).

Electrochemical measurement To prepare the cathode electrodes, active materials (80.0 wt.%), super P (10.0 wt.%), polytetrafluoroethylene (PVDF, 10 wt.%, Alfa Aesar) were dispersed in N-methyl pyrrolidone (NMP, anhydrous, 99.5%, packaged under argon) solvent. All materials were blended in a blender mixer at the rotation speed of 2000 rpm for 30 min. The obtained slurry was casted on Al foil and then dried in air drying oven at 90 °C for 40 min and whereafter vacuum oven at 120 °C for 7 h to get the electrode of which the areal density of active materials was about 4 mg/cm^2. CR 2032-coin cells were assembled in a glove box filled with argon gas (99.999%), using the above-mentioned electrodes as cathode and lithium foil (500 nm) as anode. The assembled cells were cycled in the voltage range of 2.75 V–4.3 V (vs. Li/Li^+) with a current rate of 0.1 C (1 C = 200 mA/g) at 25 °C.

3. Results and discussion

Usually, the intensity ratio of $peak_{003}$ to $peak_{104}$ ($R_{(003)/(104)}$) is used to evaluate the Li/Ni mixing degree of layered materials. However, in practice, the ratio is not consistent in repeated trials due to the multiple experiment conditions, such as the difference from pressure strength of sample preparation, instrument status, preferred orientation, etc. For example, Figs. 1(a)–1(f) show the XRD patterns of the same LNO sample synthesized at 750 °C which tested at different conditions. The XRD patterns from No. 1 to No. 5 are various at scanning time, scanning rate and pressure strength of sample preparation, which are illustrated in Table S1. The No. 6 XRD patterns are recorded by adding a baffle above the XRD sample stage. Obviously, there are different $R_{(003)/(104)}$ values for different test conditions. The $R_{(003)/(104)}$ values and the Li/Ni mixing ratios obtained from Rietveld refinement without spherical harmonics of the six XRD patterns are shown in Fig. 1(g). The $R_{(003)/(104)}$ value varies from 0.87 to 1.10 for No. 1 to No. 5, and rapidly rises to 1.96 for No. 6, while Li/Ni mixing ratios vary from 8.03% to 11.3% in the samples from No. 1 to No. 5 and decrease to 3% for No. 6.

Table 1. Cell parameters refined from XRD of No. 1 to No. 5 without spherical harmonics and the relative deviations of the cell parameters.

Test number	a (Å)	c (Å)	V (Å^3)	c/a
No. 1	2.8804	14.206	102.08	4.9319
No. 2	2.8804	14.207	102.08	4.9321
No. 3	2.8801	14.204	102.04	4.9319
No. 4	2.8800	14.205	102.04	4.9322
No. 5	2.8801	14.205	102.05	4.9320
Test number	Ni_{Li}	RD_V	$RD_{c/a}$	$RD_{Ni/Li}$
No. 1	10.8%	0.02%	−0.003%	13.7%
No. 2	11.3%	0.02%	0.002%	19.0%
No. 3	9.17%	−0.02%	−0.003%	−3.45%
No. 4	8.03%	−0.02%	0.003%	−15.5%
No. 5	8.19%	−0.01%	0.001%	−13.8%

The cell parameters refined from the five XRD patterns (No. 1 to No. 5) without spherical harmonics are displayed in Table 1. To evaluate the deviation, the relative deviation (RD) of V (unit cell volume), c/a and Ni_{Li} (Li/Ni mixing) of every test are calculated and denoted as RD_V, $RD_{c/a}$ and $RD_{Ni/Li}$. By comparing these relative deviations, it's obvious that $RD_{c/a}$ is least and less than 0.02% and RD_V is also relatively small, while $RD_{Ni/Li}$ is generally about 10%–20%. The larger variation of $RD_{Ni/Li}$ (up to 64%) of all the six XRD patterns is due to the much smaller Li/Ni mixing degree obtained from

the No. 6 test, as shown in Table S2. These results demonstrate that the Li/Ni mixing degree obtained from Rietveld refinement without spherical harmonics is very inconsistent with test conditions, contrast to other cell parameters such as c/a and unit cell volume.

The relationship between Li/Ni mixing and $R_{(003)/(104)}$ of No. 1 to No. 5 is analyzed in Fig. 1(h). The Li/Ni mixing demonstrates a strong linear relationship with $R_{(003)/(104)}$ value, which indicates that the inconsistent $R_{(003)/(104)}$ potentially leads to the inaccurate Li/Ni mixing degree obtained from Rietveld refinement. The similar relationship of No. 1 to No. 6 is shown in Fig. S3. The No. 6 has a very low Li/Ni mixing ratio and a very small $R_{(003)/(104)}$ contrast to No. 1 to No. 5, which illustrates that $R_{(003)/(104)}$ significantly influences the obtained Li/Ni mixing degree. A baffle is used in the No. 6 test and can reduce the peak strength more seriously at higher angles and lead to a much higher $R_{(003)/(104)}$ value, which may be the main reason for the large deviation of Li/Ni mixing degree.

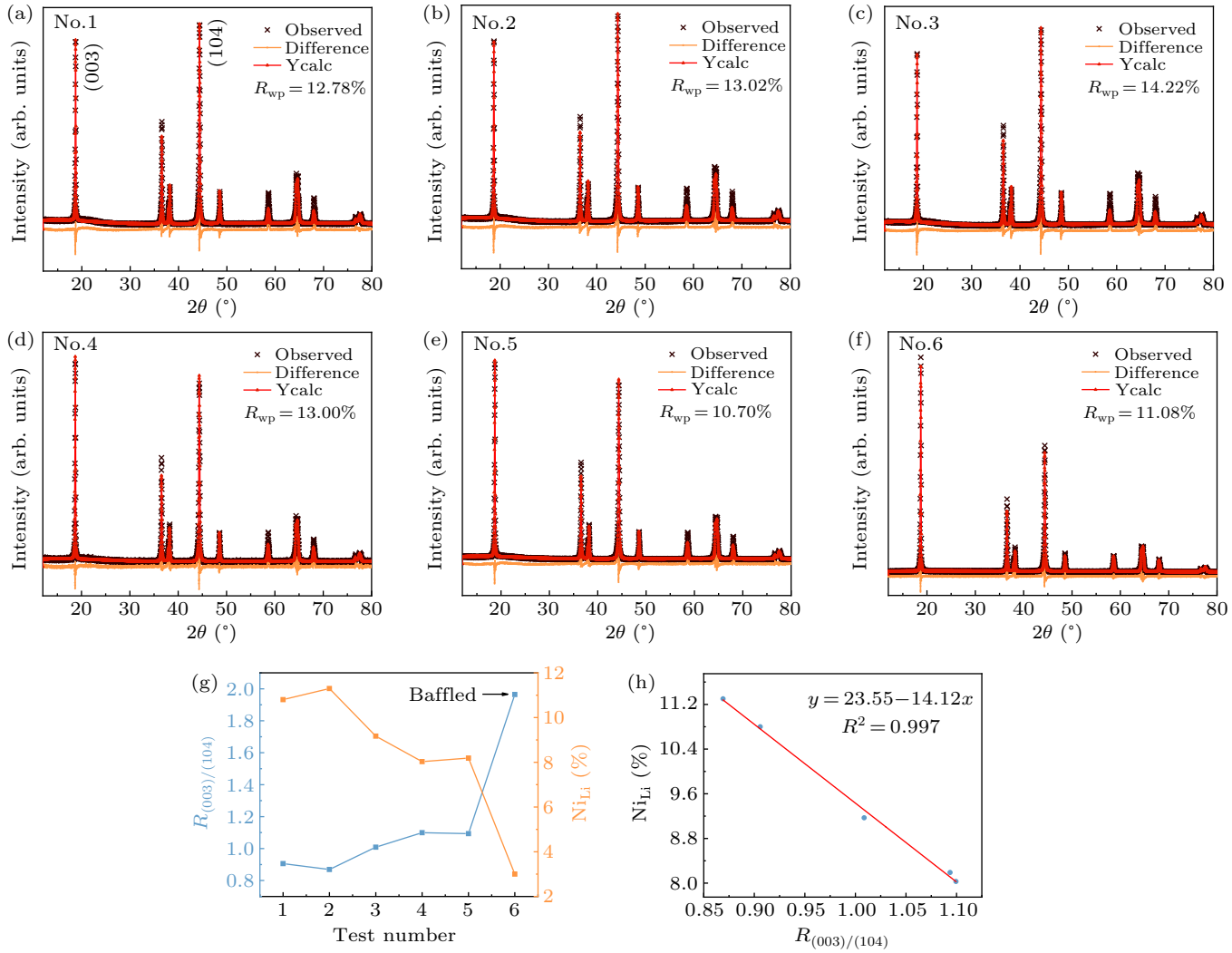


Fig. 1. Panels (a)–(f) show the XRD patterns and refinement of LNO sintered at 750 °C under different test conditions, (g) the $R_{(003)/(104)}$ and Li/Ni mixing ratios of No. 1 to No. 6, (h) the relationship between Li/Ni mixing ratio and $R_{(003)/(104)}$.

Therefore, the estimation of Li/Ni mixing degree is much influenced by the sample testing inconsistencies in practice. To accurately determine the Li/Ni mixing degree, it is necessary to eliminate the influence of sample testing inconsistencies on the peak intensities and fit the preferred orientation. In the following, we will analyze the origins of sample testing inconsistencies and discuss the methods for error reduction.

A fundamental requirement for the x-ray diffraction phenomenon is that the normal vector of a crystal plane (*hkl*), $\boldsymbol{N}_{hkl}$, is parallel to the wavevector difference ($\boldsymbol{k} - \boldsymbol{k}_0$). Only the particles which meet this requirement contribute to the peak intensity of the crystal plane (*hkl*). In theory, only perfect spheres are randomly distributed and have consistent contribution from all crystal planes to peak intensity (shown in Fig. 2(a)). However, powders usually have different and non-spherical shapes (such as an extreme case as shown in Fig. 2(b)). Under the influence of gravity, pressure, and intrinsic preferred orientation, the normal vector of certain planes is

more likely to be parallel to the direction of $(\boldsymbol{k}-\boldsymbol{k}_0)$, making these planes exhibit higher peak intensity while some planes display lower peak intensity. As a result, some diffraction peaks are enhanced, while others are weakened, which is known as the preferred orientation (texture).

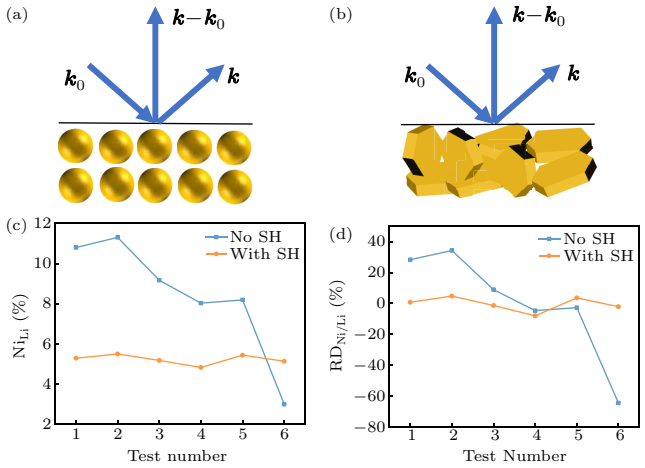


Fig. 2. (a) Schematic diagram for diffraction of perfect spheres, (b) schematic diagram for diffraction of realistic particles (just one example), (c) the refined Li/Ni mixing degree with SH and without SH of No. 1 to No. 6 tests, (d) the obtained $RD_{Ni/Li}$ with SH and without SH of No. 1 to No. 6 tests.

Spherical harmonics function (SH) is a universal method to fit the preferred orientation in previous researches,[20–23] which has not been reported in the field of LIBs. The detailed theoretical fundamental is clarified in supplementary information Part I. The results and analysis of the Rietveld refinement using SH to eliminate the preferred orientation are displayed in Table S3. The Li/Ni mixing ratios obtained from Rietveld refinement with and without SH are shown in Fig. 2(c). The Li/Ni mixing ratio with SH is about 5%, which is more consistent than that without SH. The $RD_{Ni/Li}$ with SH is much smaller than $RD_{Ni/Li}$ without SH, as shown in Fig. 2(d). The plot between Li/Ni mixing ratios and $R_{(003)/(104)}$ values of the refinement results with SH is shown in Fig. S4 and no obvious linear relationship can be obtained. These results jointly prove that the used SH can obviously reduce the disturbance from the sample testing inconsistencies and decrease the error of the refined Li/Ni mixing ratio.

Using the method of accurately determining the Li/Ni mixing degree, the relationship between the structure and electrochemical behavior of different samples is further studied. LNO and Ni92 cathode prepared with different sintering processes are characterized and the acquired XRD and SEM data are shown in Figs. S5–S8. The mean size of the primary particles of these samples is 0.3 μm–3 μm and these materials mainly are layered phase and have no impurities. The corresponding cell parameters, discharge capacity and coulombic efficiency of 1st cycle are listed in Table S4.

Figure 3(a) displays the first charge and discharge curves of LNO at 25 °C with a current rate of 0.1 C. The LNO with a higher capacity generally exhibits higher Coulombic efficiency which corresponds to less Li/Ni mixing, as shown in Fig. 3(a) and Table S4.[14] The correlation between the first-cycle discharge capacity and Li/Ni mixing ratio without SH is illustrated in Fig. 3(b) and the coefficient of determination is $R^2 = 0.785$, demonstrating a weak linear relationship. After SH is employed, the coefficient of determination R^2 increases to 0.976 as shown in Fig. 3(c), indicating a much stronger linear correlation.

Similarly, the first charge and discharge curves of Ni92 at 25 °C are displayed in Fig. 3(d). The relationship between the first-cycle discharge capacity and Li/Ni mixing ratio with SH is illustrated in Fig. 3(e), which also exhibits an obvious linear correlation.

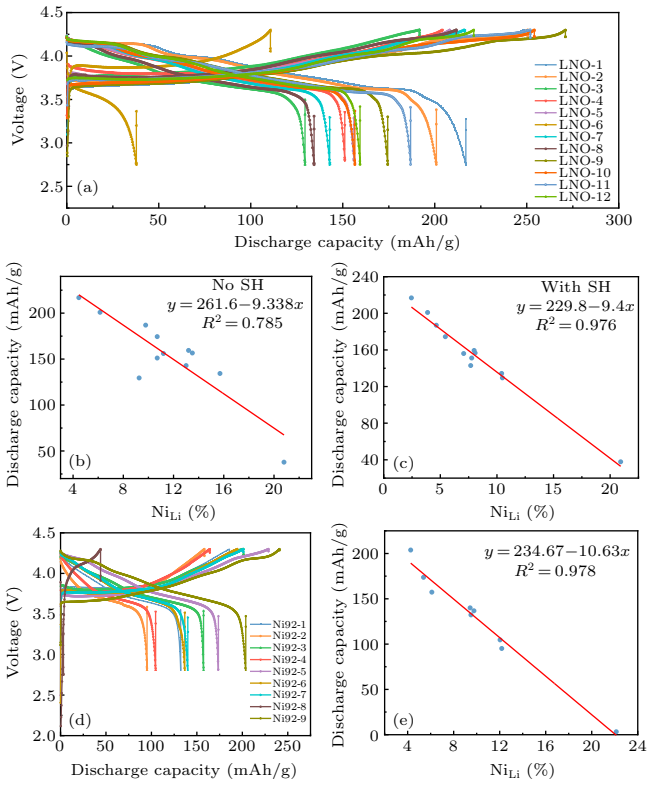


Fig. 3. (a) The first-cycle charge and discharge curves of LNO at 25 °C, (b) the relationship between 1st cycle discharge capacity of LNO and Li/Ni mixing ratio without SH, (c) the relationship between 1st cycle discharge capacity of LNO and Li/Ni mixing with SH, (d) the 1st cycle charge and discharge curves of Ni92 at 25 °C, (e) the relationship between discharge capacity of Ni92 and Li/Ni mixing with SH.

In short, the Li/Ni mixing ratio and discharge capacity demonstrate a strong correlation for LNO and Ni92. For the electrochemical testing conditions in this study, the discharge capacity decreases about 10 mAh/g when the Li/Ni mixing ratio increases 1%. However, it is difficult to directly conclude that the Li/Ni mixing leads to the worse capacity because the discharge capacity of the cathode materials is generally affected by both of bulk phase and surface phase. Therefore, the surface of these samples is analyzed further.

Raman experiments which can obtain the crystal structure information on the surface of the sample at a depth of about

10 nm, are conducted on partial samples, as shown in Fig. 4. For rock-salt structure, the Raman spectra only display a wide peak from 400 cm^{-1} to 600 cm^{-1}. For layered structure, the wide peak is divided into 2 sharp peaks named E_g and A_{1g}, and located at 465 cm^{-1} and 545 cm^{-1} respectively.[24,25] For materials with high Li/Ni mixing ratios like Ni92-8 and LNO-6, the two divided peaks of E_g and A_{1g} are not clear. With the decrease of Li/Ni mixing ratio, the splitting degree of the two peaks increases. These results indicate that the surface structure is consistent with the bulk materials. After ruling out the possibility of worse electrochemically-inactive properties of the rock-salt phase, it can be concluded that the discharge capacity of LNO and Ni92 is mainly related to the bulk phase and Li/Ni mixing directly leads to the discharge capacity loss in this study.

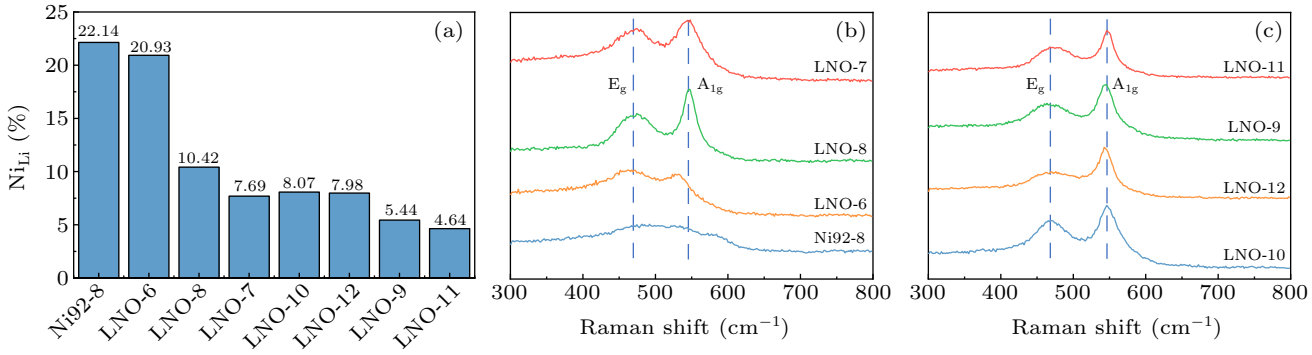


Fig. 4. (a) The Li/Ni mixing of some samples which indicate the disorder degree of the bulk, (b) and (c) the Raman spectra of these samples which show the disorder degree of the surface.

4. Conclusion

We testify the influence of sample testing conditions on the measurement of the Li/Ni mixing degree. We provide a method for more accurately determining the Li/Ni mixing degree through the employment of the spherical harmonics function, which reduces the error from sample testing inconsistencies in lab-based XRD measurements. On this basis, the accurate Li/Ni mixing ratios exhibit a notable correlation with the discharge specific capacities for LNO and Ni92. Therefore, the discharge capacity of LNO and high Ni ternary cathode materials can be estimated according to the Li/Ni mixing degree before electrochemical characterization. Our research provides an accurate method to estimate Li/Ni mixing degree adapting to various testing conditions, which is valuable to the structural analysis and rapid screening of the LNO and high-nickel ternary cathode materials.

Acknowledgments

Project supported by the Natural Science Foundation of Beijing (Grant No. Z200013), the Beijing Municipal Science & Technology (Grant No. Z191100004719001), and the National Natural Science Foundation of China (Grant Nos. 52325207 and 22005333).

References

[1] Lee J, Kitchaev D A, Kwon D H, Lee C W, Papp J K, Liu Y S, Lun Z, Clément R J, Shi T, McCloskey B D, Guo J, Balasubramanian M and Ceder G 2018 *Nature* **556** 185
[2] Ji H, Wu J, Cai Z, Liu J, Kwon D H, Kim H, Urban A, Papp J K, Foley E, Tian Y, Balasubramanian M, Kim H, Clément R J, McCloskey B D, Yang W and Ceder G 2020 *Nat. Energy* **5** 213
[3] Li W, Erickson E M and Manthiram A 2020 *Nat. Energy* **5** 26
[4] Wang C, Wang X, Zhang R, Lei T, Kisslinger K and Xin H L 2023 *Nat. Mater.* **22** 235
[5] Tan S, Shadike Z, Li J, Wang X, Yang Y, Lin R, Cresce A, Hu J, Hunt A, Waluyo I, Ma L, Monaco F, Cloetens P, Xiao J, Liu Y, Yang X Q, Xu K and Hu E 2022 *Nat. Energy* **7** 484
[6] Park K J, Jung H G, Kuo L Y, Kaghazchi P, Yoon C S and Sun Y K 2018 *Adv. Energy Mater.* **8** 1801202
[7] Wang L, Liu T, Wu T and Lu J 2022 *Nature* **611** 61
[8] Sun Y, Liao J, Zhang H, Song D, Wang D and Zhang L 2023 *J. Power Sources* **563** 232774
[9] Kaneda H, Furuichi Y, Ikezawa A and Arai H 2022 *ACS Appl. Mater. Interfaces* **14** 52766
[10] Wang C, Yu R, Hwang S, Liang J, Li X, Zhao C, Sun Y, Wang J, Holmes N, Li R, Huang H, Zhao S, Zhang L, Lu S, Su D and Sun X 2020 *Energy Stor. Mater.* **30** 98
[11] Kong X, Zhang Y, Peng S, Zeng J and Zhao J 2020 *ACS Sustain. Chem. Eng.* **8** 14938
[12] Li H, Li J, Zaker N, Zhang N, Botton G A and Dahn J R 2019 *J. Electrochem. Soc.* **166** A1956
[13] Fan X M, Huang Y D, Wei H X, Tang L B, He Z J, Yan C, Mao J, Dai K H and Zheng J C 2022 *Adv. Funct. Mater.* **32** 2109421
[14] Delmas C, Pérès J P, Rougier A, Demourgues A, Weill F, Chadwick A, Broussely M, Perton F, Biensan P H and Willmann P 1997 *J. Power Sources* **68** 120
[15] Zhang J, Zhou D, Yang W, Yang J, Sun L, Schumacher G and Liu X 2019 *J. Electrochem. Soc.* **166** A4097
[16] Shen J, Zhang B, Huang W, Li X, Xiao Z, Wang J, Zhou T, Wen J, Liu T, Amine K and Ou X 2023 *Adv. Funct. Mater.* **33** 2300081
[17] Bianchini M, Roca-Ayats M, Hartmann P, Brezesinski T and Janek J 2019 *Angew. Chem. Int. Ed.* **58** 10434
[18] Qian G, Li Z, Meng D, Liu J, He Y S, Rao Q, Liu Y, Ma Z F and Li L 2021 *J. Electrochem. Soc.* **168** 010534
[19] Song J, Zhu L, Li Y, Han E, Zhang Q, Chen G, Zhang Z, Yang X and He Y 2023 *J. Electrochem. Soc.* **170** 010523
[20] Whitfield P S 2009 *J. Appl. Crystallogr.* **42** 134
[21] Bergmann J, Monecke T and Kleeberg R 2001 *J. Appl. Crystallogr.* **34** 16
[22] Järvinen M 1993 *J. Appl. Crystallogr.* **26** 525
[23] Ahtee M, Nurmela M, Suortti P and Järvinen M 1989 *J. Appl. Crystallogr.* **22** 261
[24] Yang L, Zhang J, Xue W, Li J, Chen R, Pan H, Yu X, Liu Y, Li H, Chen L and Huang X 2022 *Adv. Funct. Mater.* **32** 2200096
[25] Inaba M, Iriyama Y, Ogumi Z, Todzuka Y and Tasaka A 1997 *J. Raman Spectrosc.* **28** 613